AD_____

Award Number: W81XWH-11-1-0716

TITLE: Development of a Novel Synthetic Drug for Osteoporosis and Fracture Healing

PRINCIPAL INVESTIGATOR:　　　　Hiroki Yokota, Ph.D.

CONTRACTING ORGANIZATION:　　Indiana University
　　　　　　　　　　　　　　　　　　　　　Indianapolis, IN 46202

REPORT DATE:　　　September　2012

TYPE OF REPORT:　Annual

PREPARED FOR:　U.S. Army Medical Research and Materiel Command
　　　　　　　　　　　Fort Detrick, Maryland　21702-5012

REPORT DOCUMENTATION PAGE

1. REPORT DATE	2. REPORT TYPE	3. DATES COVERED
September 01, 2012	Annual	22 Aug 2011 - 21 Aug 2012

4. TITLE AND SUBTITLE

Development of a Novel Synthetic Drug for Osteoporosis and Fracture Healing

5a. CONTRACT NUMBER

W81XWH-11-1-0716

5b. GRANT NUMBER

5c. PROGRAM ELEMENT NUMBER

6. AUTHOR(S)

Hiroki Yokota, Ph.D.

E-Mail: hyokota@iupui.edu

5d. PROJECT NUMBER

5e. TASK NUMBER

5f. WORK UNIT NUMBER

7. PERFORMING ORGANIZATION NAME(S) AND ADDRESS(ES)
Indiana University
Indianapolis, IN 46202

8. PERFORMING ORGANIZATION REPORT NUMBER

9. SPONSORING / MONITORING AGENCY NAME(S) AND ADDRESS(ES)
U.S. Army Medical Research and Materiel Command
Fort Detrick, Maryland 21702-5012

10. SPONSOR/MONITOR'S ACRONYM(S)

11. SPONSOR/MONITOR'S REPORT NUMBER(S)

12. DISTRIBUTION / AVAILABILITY STATEMENT
Approved for Public Release; Distribution Unlimited

13. SUPPLEMENTARY NOTES

14. ABSTRACT

This is a progress report (year 1) for developing a novel therapeutic drug for skeletal diseases, in particular focusing on administration of salubrinal for treatment of osteoporosis and bone fracture. A formulation for salubrinal was determined and an effective dosage was identified. Using ovariectomized mice, administration of salubrinal was shown to reduce body weight and fat weight, and to prevent reduction in uterus weight and BMD/BMC. Salubrinal was also shown to inhibit osteoclast development and to stimulate osteoblast development through regulation of key transcription factors such as ATF4, $NF\kappa B$, and NFATc1. A pathway analysis revealed that the observed effects of salubrinal were mediated by $eIF2\alpha$, p38 MAPK, and $NF\kappa B$ pathways. Multiple invention disclosures and patents were submitted or being prepared for bone remodeling, fat metabolism, joint preservation, cancer treatment, and salubrinal coating on transplantable materials. A collaborative relationship was established with Zimmer Co. Two research abstracts were submitted, two peer-reviewed articles are in press, and one peer-reviewed research article was submitted.

15. SUBJECT TERMS U]^\åæ\↔´ÁŒã|&ÊŠb\æ~*~ã~b↔bÊÔãá´\|ãæ Healing

16. SECURITY CLASSIFICATION OF:			17. LIMITATION OF ABSTRACT	18. NUMBER OF PAGES	19a. NAME OF RESPONSIBLE PERSON USAMRMC
a. REPORT	b. ABSTRACT	c. THIS PAGE			
U	U	U	UU	21	19b. TELEPHONE NUMBER (include area code)

Table of Contents

Introduction
This is a first-year progress report of the project (W81XWH-11-1-0716; Development of a novel synthetic drug for osteoporosis and fracture healing). The project aims at developing a novel synthetic drug for osteoporosis and healing of bone fracture, and a particular focus is placed on evaluation of salubrinal, a chemical agent ($C_{21}H_{17}Cl_3N_4OS$, 480 Da), as a novel synthetic drug. In the year one, we conducted investigations on part of Aims 1 and 2:

- Aim 1 (Development of salubrinal formulations and determination of pharmacodynamics)
- Aim 2 (Evaluations of efficacy of salubrinal on bone formation).

This progress report documents the results obtained in the first year on these two aims. The results include evaluation of salubrinal formulations, solubility of salubrinal in simulated physiological fluids, concentration of salubrinal in mouse serum, subcutaneous administration of salubrinal to normal mice, effects of salubrinal on body weight and uterus in ovariectomized mice, effects of salubrinal on fat metabolism, bone mineral density (BMD) and bone mineral content (BMC), effects of salubrinal on development of osteoclasts, effects of salubrinal on migration and adhesion of osteoclasts, effects of salubrinal on colony-forming unit-macrophage/monocyte (CFU-M), effects of salubrinal on osteoblast differentiation, effects of salubrinal on osteoblast and osteocyte apoptosis, effects of salubrinal on colony-forming unit fibroblasts (CFU-F), *in vitro* effects of salubrinal on osteoclast precursor cells, *in vitro* effects of salubrinal on osteoblasts, *in vitro* effects of salubrinal on chondrocytes, application to chondrosarcoma, and preparation for bone fracture study.

Body
Aim 1: Development of salubrinal formulations and determination of pharmacodynamics
Evaluation of salubrinal formulations: A formulation screen was performed for the purpose of identifying conditions compatible with injection and oral administration with satisfactory salubrinal solubility. A total of 25 vehicles were prepared in 10 or 20 mM phosphate buffer or water, including a selection of surfactants, co-solvents, and complexing agents. Most vehicles were prepared at physiological pH. A pH 3.0 phosphate buffer was included in the screen to evaluate the effect of pH on salubrinal solubility. Samples were prepared to a target salubrinal concentration of 15 mg/mL and incubated overnight at ambient temperature on a rotator. After 24 hours, the samples were centrifuged and the supernatant analyzed by HPLC.

A rapid, stage-appropriate HPLC-UV method was developed for the quantitation of salubrinal concentration in solution. A UV scan from 200 to 800 nm was performed using a 0.1 mg/ml solution of the API in methanol to determine the best wavelength for the assay, which was identified at 276 nm. A reasonable peak shape was obtained with phenyl stationary phase, and the method was optimized to achieve an acceptable retention time. A representative chromatogram for the final method is shown in Figure 1. No further optimization was performed. The quantification of salubrinal solution concentration in the subsequent studies was carried out relative to a single external standard containing 0.1 mg/mL salubrinal, using an average peak area of triplicate injections. We examined a combination of the following chemicals at various concentrations:

EtOH	ethanol	PG	propylene glycol
PEG	polyethylene glycol	DMA N	N-dimethylacetamide
PVP	polyvinyl pyrrolidone	HPMC	hydroxypropyl methylcellulose
HPβCD	hydroxypropyl-β-cyclodextrin.		
TPGS	vitamin E d-α-tocopheryl polyethylene glycol 1000 succinate		

The samples diluted in simulated gastric fluid (SGF) were re-suspended by vortex agitation and diluted 1:10 into simulated intestinal fluid (SIF), pH 6.8, which was prepared to USP specifications and contained pancreatin. The samples were agitated on a rotator for 15 minutes. The resultant mixtures were centrifuged, a portion of the supernatant was removed and the pancreatin was precipitated with two volumes of acetonitrile. The samples were centrifuged again and supernatant was analyzed by HPLC. The results are presented in Table 1. The greatest solubility of salubrinal was achieved in vehicles containing PEG 400 and TPGS.

Solubility of salubrinal in simulated physiological fluids: Seven formulations were identified with salubrinal concentrations from 0.3 to 1.8 mg/ml (Table 2). A number of vehicles suitable for i.v. and oral administration of salubrinal were prepared with satisfactory active pharmaceutical ingredients (API) concentration and recovery upon dilution into simulated physiological fluids. The vehicles may be ranked based on their concentration in

vehicle, composition, and performance in these *in vitro* tests. In the absence of the *in vitro/in vivo* correlation, all parameters are considered equally important. The correlation between the *in vitro* data sets and performance *in vivo* (IVIVC) will have to be established as the project progresses into the animal testing phase. Of these, four are appropriate for IV administration and six for oral administration. The samples were subsequently diluted into simulated plasma and simulated gastric and intestinal fluids, as appropriate, and were analyzed for percent recovery of API in solution.

Table 1. Salubrinal formulations in simulated gastric fluid (SGF).

The samples diluted in SGF were re-	Vehicle Description (% w/w)1	API in SGF, µg/mL	Theoretical API in SIF, µg/mL2	Calculated API in SIF, µg/mL	% Recovery of SGF	Precipitate observed on
1	20% EtOH	0.05	0.005	0.1	≥100	Yes
2	50% PG	1.2	0.1	0.2	≥100	Yes
3	50% PEG 400	30.1	2.7	0.3	12.1	Yes
4	30% Glycerin	0.0	0.0	0.0	0.0	Yes
5	19.5 % EtOH, 0.5% Tween 80	1.8	0.2	0.1	51.7	Yes
6	49.5% PG, 0.5% Tween 80	6.7	0.6	0.4	64.1	Yes
7	**49.5% PEG 400, 0.5% Tween 80**	**54.4**	**4.9**	**2.7**	**53.6**	Yes
8	29.5% glycerin, 0.5% Tween 80	4.9	0.4	0.2	54.3	Yes
10	**20% EtOH, 5% TPGS**	**29.5**	**2.7**	**2.0**	**73.6**	Yes
11	18% EtOH, 2% PVP K-15	0.2	0.0	0.0	≥100	Yes
13	**45% PG, 5% TPGS**	**87.7**	**8.0**	**6.8**	**85.4**	Yes
14	48% PG, 2% PVP K-	2.2	0.2	0.0	0.0	Yes
16	**45% PEG 400, 5% TPGS**	**168.2**	**15.3**	**13.9**	**90.9**	Yes
17	48% PEG 400, 2% PVP K-15	31.6	2.9	0.4	15.3	Yes
18	10 mM pH 7.4 phosphate buffer	0.0	0.0	0.0	––	Yes
19	10 mM pH 3.0 phosphate buffer	0.0	0.0	0.0	---	Yes
20	0.25% methylcellulose in water	0.0	0.0	0.0	––	Yes
21	0.5% HPMC in	0.0	0.0	0.0	---	Yes
22	10% HPβCD in 10 mM pH 7.4 phosphate buffer	0.6	0.1	0.0	0.0	Yes
23	30% HPβCD in 10 mM pH 7.4 phosphate	3.6	0.3	0.0	0.0	Yes

Table 2. Seven formulations identified with salubrinal concentrations from 0.3 to 1.8 mg/ml.

Sample #	Vehicle Description (% w/w in 10 mM pH	Conc. API at 24 h, µg/mL	Apparent pH at 24 h	% Recovery in SB	% Recovery in SGF	% Recovery in SIF
3	50% PEG 400	330.8	8.5	65.3	62.5	12.1
7	49.5% PEG 400, 0.5% Tween 80	598.4	8.3	80.4	76.1	53.6
10	20% EtOH, 5% TPGS	324.9	7.7	n/a	82.4	73.6
13	45% PG, 5% TPGS	965.2	7.9	n/a	75.3	85.4
15	48% PEG 400, 2% DMA	427.5	8.4	81.9	n/a	n/a
16	45% PEG 400, 5% TPGS	1849.9	8.2	n/a	0.0	90.9
17	48% PEG 400, 2% PVPK K 15	347.1	7.9	79.6	78.0	15.3

Samples 10, 13, and 16 are identified for oral administration only, while the sample 15 for injection only. Samples 3, 7, and 17 are for both oral administration and injection. Since API of the sample 7 (49.5% PEG400 and 0.5% Tween 80) is the highest among three samples, we decided to use the formulation of this sample hereafter.

Concentration of salubrinal in mouse serum: Using the formulation identified above, we administered salubrinal by three different routes (SC- subcutaneous, IP – intraperitoneal, and OR – oral gavage) and determined the concentration of salubrinal in serum. The dosage of salubrinal was 1.25 mg/kg per administration, and blood was drawn at 0 h (prior to administration), 0.5 h, 1 h, 2 h, 4 h, and 8 h. The concentration of salubrinal in serum was determined using mass spectrometry (Figs. 1-3).
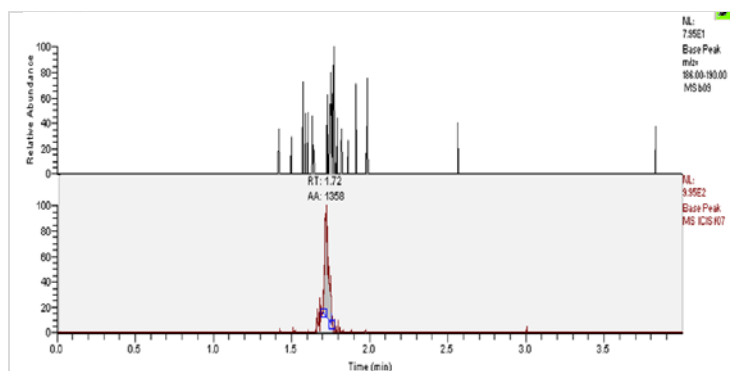

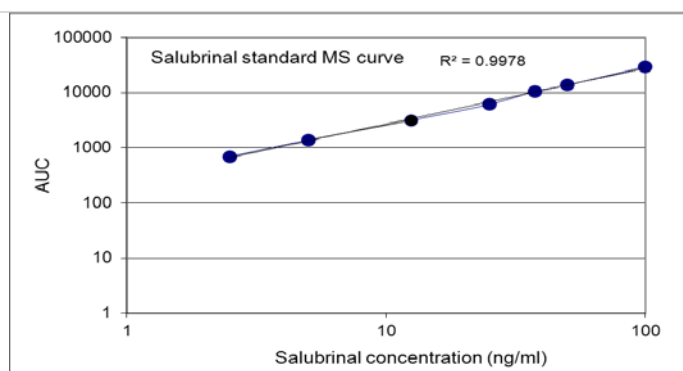Figure 1. Ion chromatogram of salubrinal detection.

Figure 2. Standard mass spec curve for determining the concentration of salubrinal.
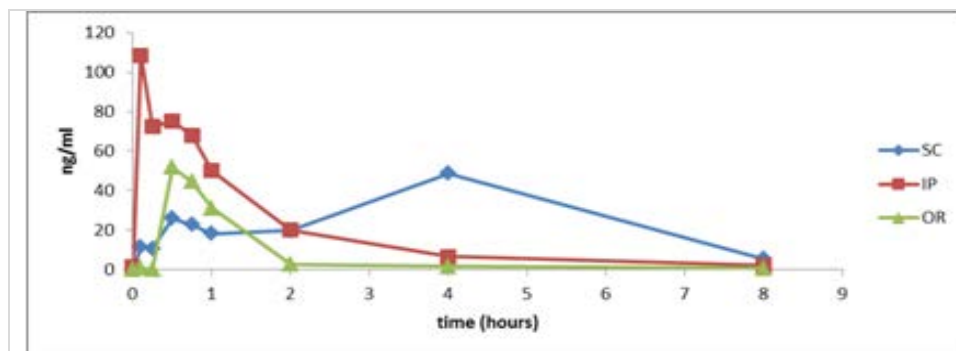

Figure 3. Concentration of salubrinal in serum after administration by three different routes (SC: subcutaneous; IP: intraperitoneal, and OR: oral gavage). Each point represents the average of three measures.

Note that propylene glycol was identified as an excellent solvent of salubrinal, but this agent is a hazardous chemical and we did not use it as a standard formulation.

Aim 2: Evaluations of efficacy of salubrinal on bone formation

Subcutaneous administration of salubrinal to normal mice (12 wk old): Using C57/B6 mice (~ 12 weeks, female) we first conducted a pilot study to determine appropriate dosage for subcutaneous administration. The selected set of dosages was 0.005, 0.025, 0.05, and 0.25 mg/kg per day. At 2, 4, and 6 weeks after initiation of daily injection of salubrinal, bone mineral density (BMD) was determined using PIXImus (Fig. 4). Except for the response to the highest dosage of 0.25 mg/kg, no significant increase in BMD was observed compared to vehicle controls. Thus, we decided to increase dosages and re-examined the responses to salubrinal administered at 0.25, 0.75, and 1.25 mg/kg (Fig. 5).
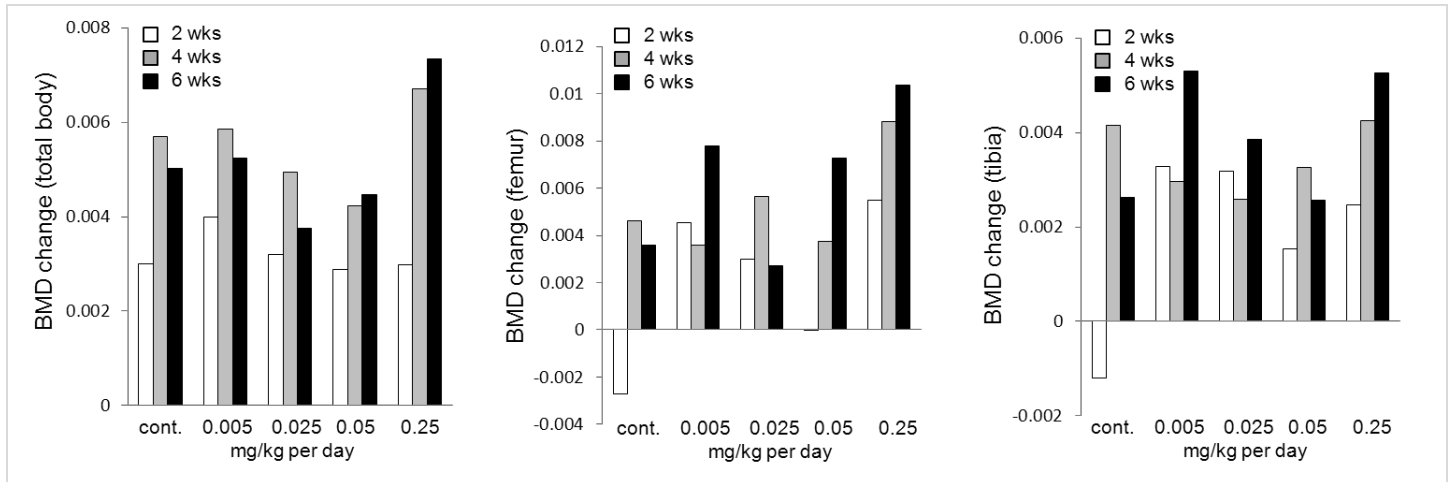

Figure 4. Changes in BMD g/cm^2 (total body, femur, and tibia) by subcutaneous administration of salubrinal (0.005, 0.025, 0.05, and 0.25 mg/kg body weight).

Compared to vehicle controls, the highest dosage at 1.25 mg/kg led to elevation in BMD of whole body, spine, and femur. However, no clear dosage response was observed. We also evaluated the effects of salubrinal on fat metabolism (Fig. 5D). Preliminary data indicate that salubrinal reduces % whole body fat. Using microCT, we reconstructed 3D images of trabecular bone in the spine and those of cortical bone in the femur, re-evaluating BMD and other bone morphometric parameters. The assessment is still underway. In addition, we took an alternative approach – induction of osteoporosis through ovariectomy and evaluation on the effects of salubrinal as shown below.
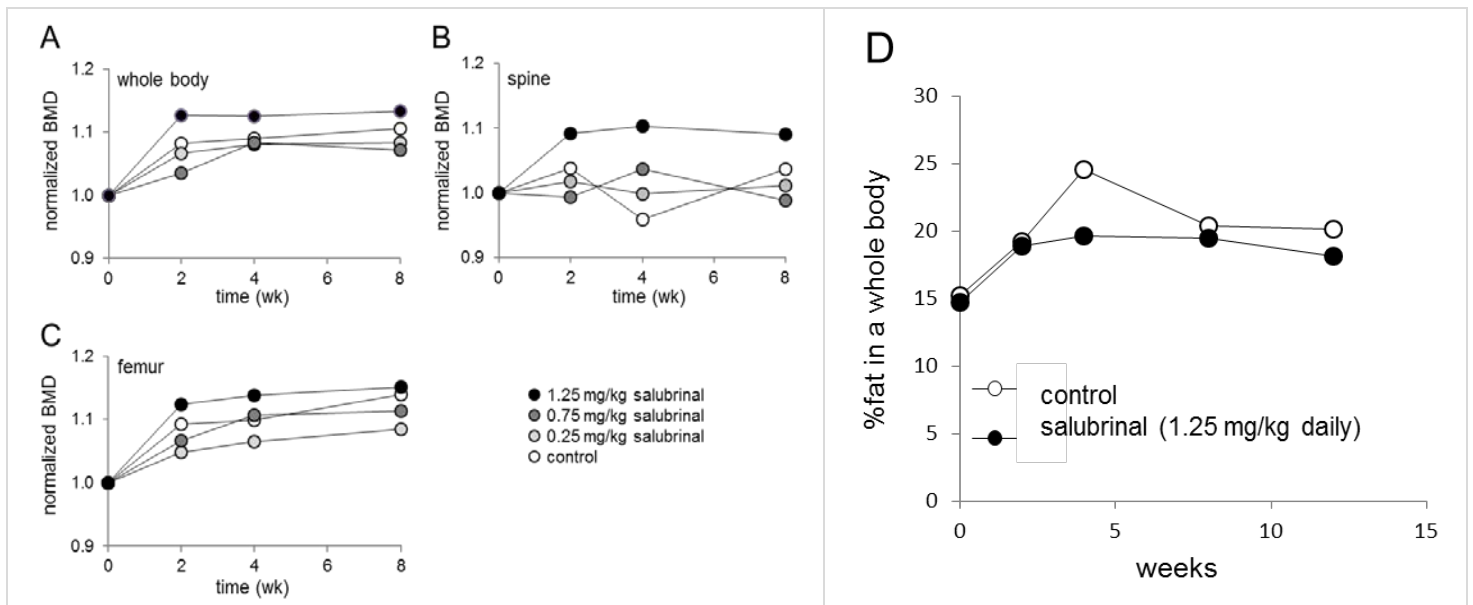

Figure 5. Normalized BMD by subcutaneous administration of salubrinal at the dosages of 0.25, 0.75, and 1.25 mg/kg. At week 0, C57/B6 mice (female) of age 12 wk were used. (A) Whole body BMD. (B) Spine BMD. (C) Femur BMD. (D) %fat in a whole body.

Effects of salubrinal on body weight and uterus in ovariectomized mice: C57/B6 mice (~ 12 week-old, female) were ovariectomized (OVX mice). In brief, mice were placed in ventral recumbency. The hair at the operative sites (dorsal mid-lumbar area) was shaved and the skin was cleaned with 70% alcohol and 10% providoneiodine solution. With the scalpel, a 10 mm skin incision was made on the midline of dorsa between the caudal edge of ribcage and the pelvis. Through the skin incision, the muscle wall of left side was incised to enter the abdominal cavity and the ovary was excised. The uterus body was placed back into the abdominal cavity. The ovary in the right side was moved in the same procedure. The wound was closed by suturing. For sham OVX mice, the same procedure was conducted but the ovaries were not removed. These mice were maintained for 4 weeks, then starting from week 5, salubrinal was subcutaneously administered at 1 mg/kg per day for the next 4 weeks. Eight weeks following ovariectomy, effects of salubrinal on OVX mice and those on sham OVX mice were evaluated.

Compared to the sham OVX mice, the OVX mice increased their body weight. Such increase in body weight, induced by ovariectomy, however, was suppressed by administration of salubrinal (Fig. 6). Ovariectomy by itself resulted in significant diminishment in size and weight of uterus. Salubrinal administration suppressed this reduction in uterus (Fig. 7).
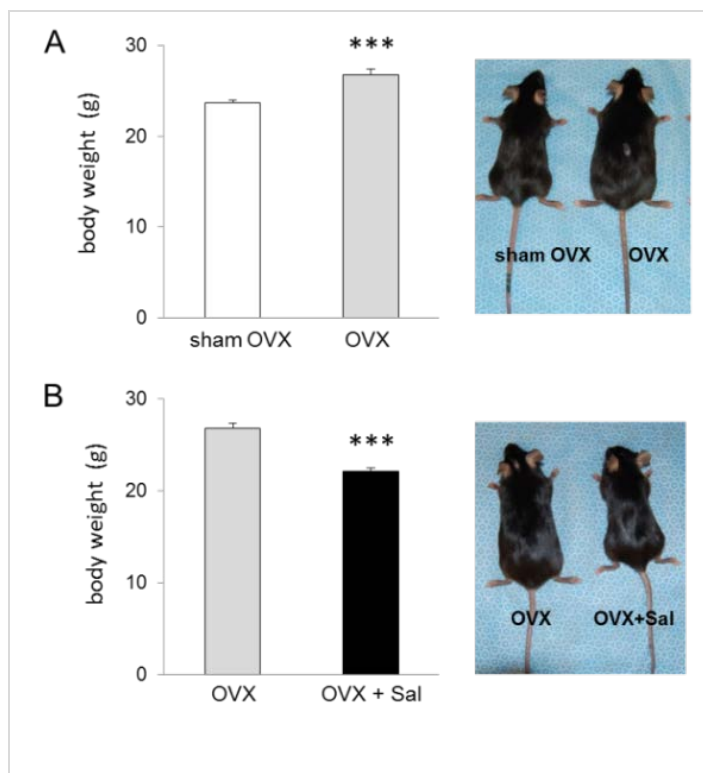

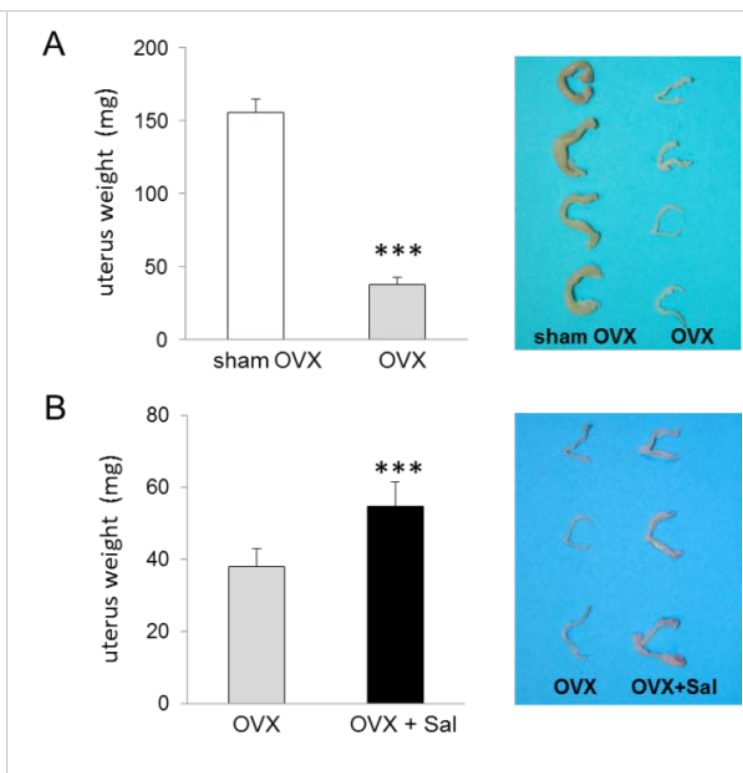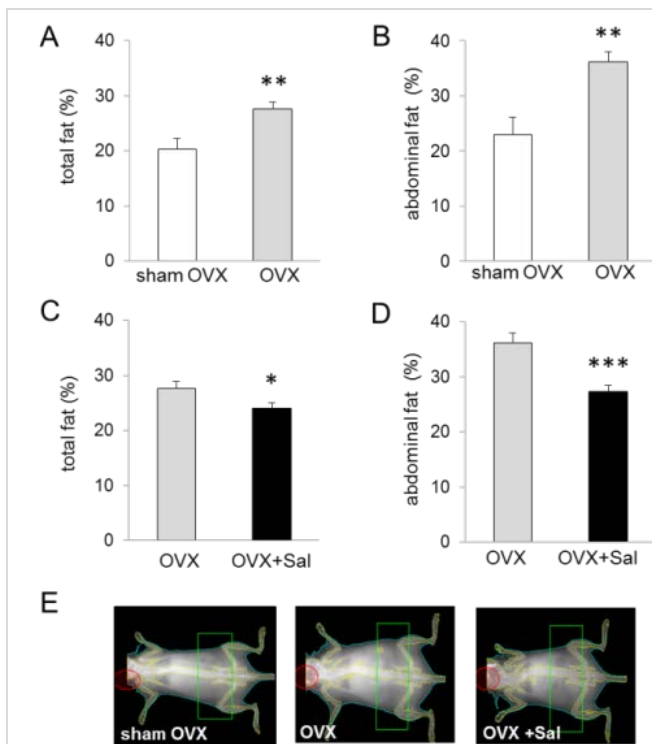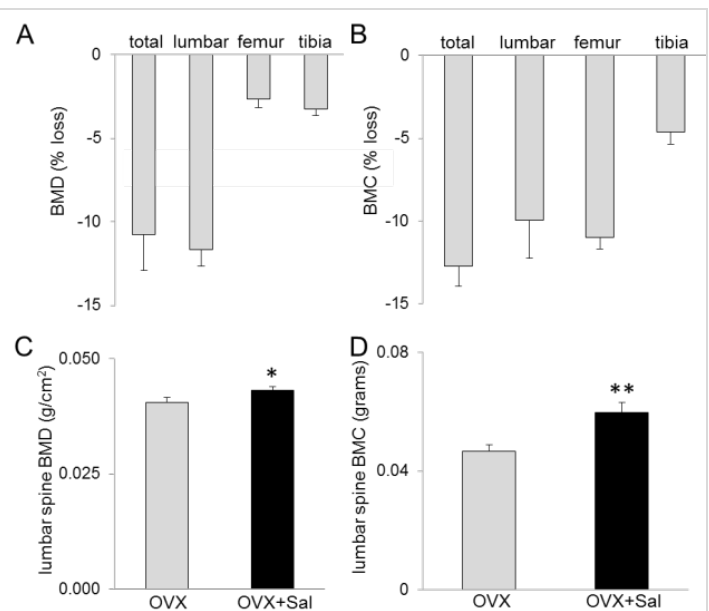| Figure 6. Effects of ovariectomy and salubrinal on body weight. (A) Gain in body weight by ovariectomy 8 weeks after surgery. (B) Reduction in body weight by subcutaneous administration of salubrinal (by 4 week checkup in the second half of the 8-week ovariectomized period) to OVX mice. | Figure 7. Effects of ovariectomy and salubrinal on uterine weight. (A) Reduction in uterine weight in OVX mice 8 weeks after ovariectomy. (B) Increase in uterine weight by subcutaneous administration of salubrinal in the second half of the 8-week ovariectomized period. |

Effects of salubrinal on fat metabolism, bone mineral density (BMD) and bone mineral content (BMC):
Ovariectomy increased body fat weight including abdominal fat. Administration of salubrinal to the OVX mice reduced fat weight of total body and abdomen (Fig. 8). PIXImus images in Fig. 8E show that the OVX mouse is larger with more fat contents than the sham OVX and salubrinal-treated OVX mice.

The OVX mice had reduc ed BMD (bone mineral density) and BMC (bone mineral content) in total body, spine, femur, and tibia. In response to subcutaneous administration of salubrinal to the OVX mice, the BMD and BMC in spine were significantly decreased (Fig. 9).

Figure 8. Effects of ovariectomy and salubrinal on body fat. Dual energy X-ray absorptiometry is used to measure total (%) and abdominal fat (%). (A) Increase in total fat (%) in the OVX mice 8 weeks after ovariectomy. (B) Increase in abdominal fat in the OVX mice. (C) Reduction in total fat (%) by 4-week administration of salubrinal in the second half of the 8-week period. (D) Decrease in abdominal fat (%) by 4-week salubrinal treatment. (E) PIXImus images.

Figure 9. Effects of ovariectomy and salubrinal on BMD and BMC. (A) Reduction in BMD (% loss) in total body, lumbar spine, femur, and tibia in the OVX mice 4 weeks after ovariectomy. (B) Reduction in BMC (%loss) in total body, lumbar spine, femur, and tibia in the OVX mice. (C) Increase in lumbar spine BMD (g/cm^2) in the salubrinal treated OVX mice. (D) Increase in BMC (g) in lumbar spine in the salubrinal treated OVX mice.

Effects of salubrinal on development of osteoclasts: To examine the mechanism of salubrinal's action on BMD and BMC of the OVX mice, we examined osteoclastogenesis of bone marrow derived cells from the sham OVX and OVX mice in the presence and absence of salubrinal.

In the first set of experiments, bone marrow cells were harvested from three groups of mice (sham OVX, OVX, and salubrinal-treated OVX mice). Murine bone marrow mononuclear cells (BMMNCs) were collected from experimental mice by flushing the iliac, femurs and tibias with Iscove's MEM containing 10% fetal bovine serum (FBS) using a 23-gauge needle. BMMNCs were then separated by low-density gradient centrifugation. BMMNCs were cultured in α-MEM supplemented with 10% FBS and 30 ng/ml murine macrophage-colony stimulating factor (M-CSF) and 20 ng/ml murine receptor activator of nuclear factor kappa-B ligand (RANKL) for 3 days. On day 3, cell culture media were switched to α-MEM supplemented with 10% FBS, M-CSF (30 ng/ml), and RANKL (60 ng/ml) for an additional 3 days of culture. Using TRACP staining, osteoclast cells were stained and the area covered by osteoclasts on the surface of culture dishes was determined (Fig. 10). The result revealed that compared to cells isolated from the sham OVX control the osteoclast area (OCL area) was significantly increased in cells from the OVX mice. This increase was not observed in cells isolated from the salubrinal-treated OVX mice (Fig. 10).

In other sets of experiments, bone marrow cells were isolated from two groups of mice (sham OVX, and OVX mice), and cells were incubated with salubrinal at 1, 2, or 5 μM from day 0 or day 4 of the culture process. The result showed that incubation with salubrinal reduced OCL area in a dose dependent manner regardless of incubation from day 0 or day 4 (Fig. 11).
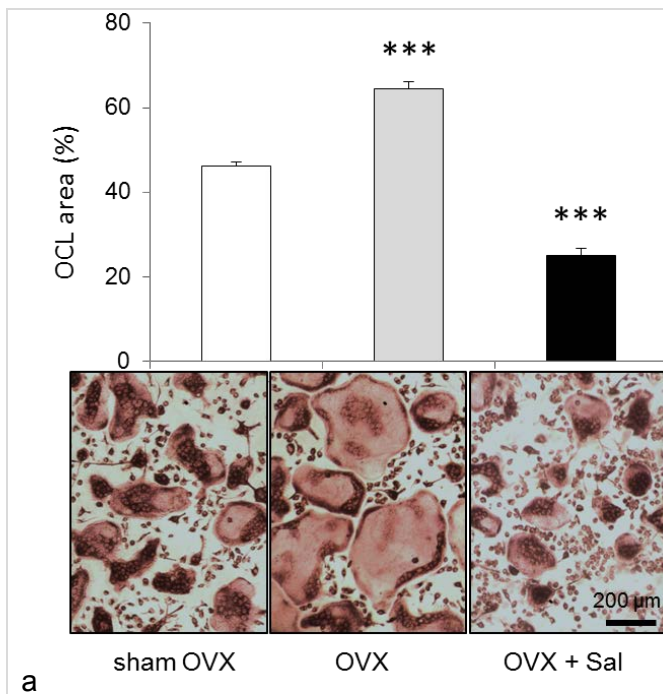
Figure 10. Suppression of osteoclast development by subcutaneous administration of salubrinal. The ratios of osteoclast areas are compared among 3 groups (sham OVX, OVX control, and salubrinal treated OVX). Data are collected 8 weeks after ovariectomy with and without subcutaneous administration of salubrinal in the second half of the 8-week period, and shown with mean ± s.e.m representing nine images (3 independent experiments and 3 images per experiment). The OVX control mice show a significant increase in the osteoclast area compared to the sham OVX, while the salubrinal treated mice significantly reduced its area compared to the sham OVX and OVX control mice. The microphotographs represent the three groups of osteoclast cultures with TRACP staining. Note that $p < 0.001$ for the salubrinal treated OVX mice vs. the OVX mice, as well as the OVX mice vs. the sham OVX mice (ANOVA followed by post-hoc t-test). Bar = 200 μm.
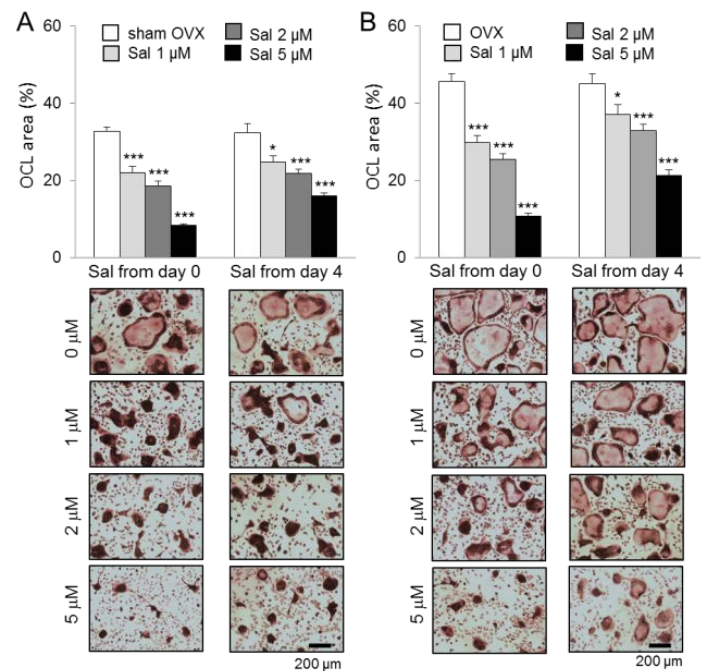
Figure 11. The effects of post administration of salubrinal in culture on osteoclast formation. Salubrinal is administered at 3 dosages (1, 2, and 5 μM). The single and triple asterisks indicate $p < 0.05$ and $p < 0.001$, respectively. Bar = 200 μm. (A) Comparison of osteoclast formation in the sham OVX mice with and without post administration of salubrinal in the isolated bone marrow cells. On the left panel, salubrinal was administered from day 0 (initiation of osteoclast culture), while on the right panel from day 4, salubrinal reduced osteoclast area (%) in both groups in a dose-dependent manner. The images on the bottom display the representative states of osteoclasts. (B) Comparison of osteoclast formation in the OVX mice with and without post administration of salubrinal in the isolated bone marrow cells. Salubrinal was administered from day 0 on the left panel and from day 4 on the right panel. Salubrinal reduced osteoclast area (%) in a dose-dependent manner.

Effects of salubrinal on migration and adhesion of osteoclasts: Using bone marrow derived cells from three groups of mice (sham OVX, OVX, and salubrinal-treated OVX mice), we next examined effects of salubrinal on migration and adhesion of osteoclasts (Fig. 12).

Migration of osteoclasts was evaluated using a transwell assay. BMMNCs previously cultured in M-CSF and RANKL for 3 days were applied for the assay of migration and adhesion. The cells were lifted from the plates by incubating with 0.05% trypsin. Equivalent numbers of TRACP+ cells were separated and loaded onto the upper chamber of transwells. They were allowed to migrate through an 8-μm polycarbonate filter coated with vitronectin for 6 hours in a humidified incubator at 37°C. In the bottom chamber, 0.1% bovine serum albumin (BSA) was supplemented in α-MEM containing M-CSF (30 ng/mL). TRACP+ cells per field-of-view were then counted using a microscope. Regarding osteoclast adhesion assay, osteoclast precursors (1×10^5 cells/ml) were placed into 96-well plates coated with 20 μg/ml vitronectin supplemented with M-CSF (30 ng/mL). After 30 min of incubation, the wells were washed with phosphate buffered saline (PBS) 3 times and fixed with 4% paraformaldehyde at room temperature for 10 to 15 minutes. Nonattached cells were gently removed with

PBS, and adherent cells to $\alpha_v\beta_3$ were fixed with crystal violet. Adherent cells were counted under the phase contract microscope.
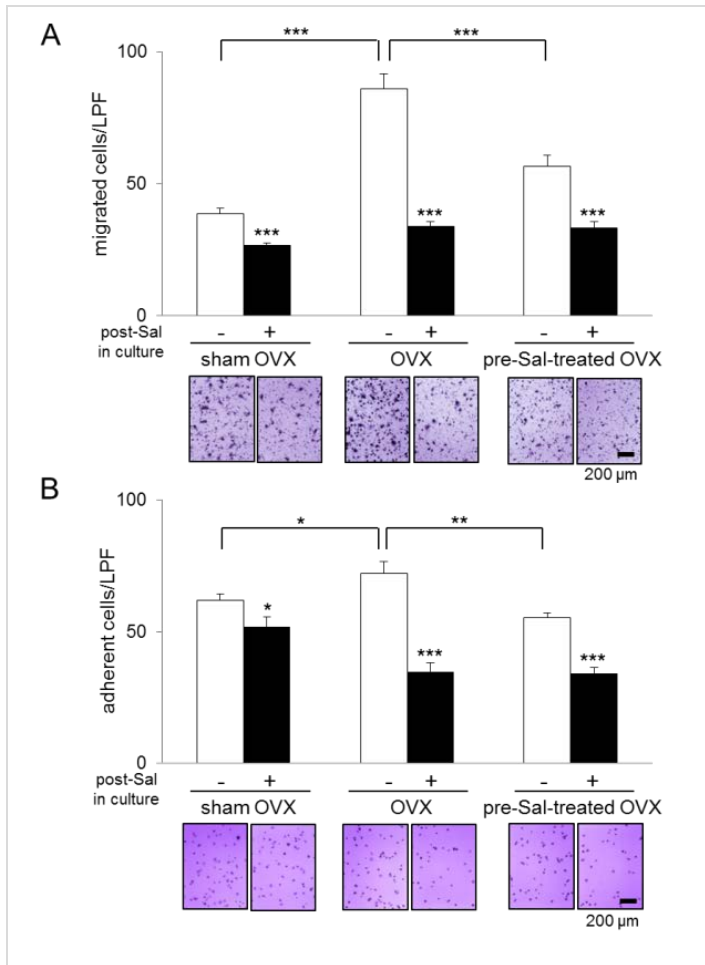
Figure 12. Effects of salubrinal on migration and adhesion of osteoclasts. (A) Haptotaxis of preosteoclasts isolated from the sham OVX, OVX, and salubrinal treated OVX mice. Bone marrow cells were isolated 8 weeks after ovariectomy. Salubrinal or vehicle was administered in the last 4 weeks. Quantitative evaluation of migration in response to M-CSF is performed in the presence and absence of post administration of salubrinal in culture using a transwell assay.   Cells isolated from OVX mice were more actively migrating than those from the sham OVX mice, and 4-week salubrinal treatment reduced migration compared to the OVX controls. The images on the bottom display 3 pairs of osteoclast cultures. Data represent mean ± s.e.m. of 10 measurements in each of three independent experiments. (B) Quantitative evaluation of M-CSF mediated preosteoclast adhesion (30 min) to $\alpha_v\beta_3$. The OVX mice presented greater adhesion than the sham OVX mice, and 4-week salubrinal treatment reduced adhesion compared to the OVX mice. Post administration of salubrinal reduced adhesion in all three groups (sham OVX, OVX, and salubrinal treated OVX).
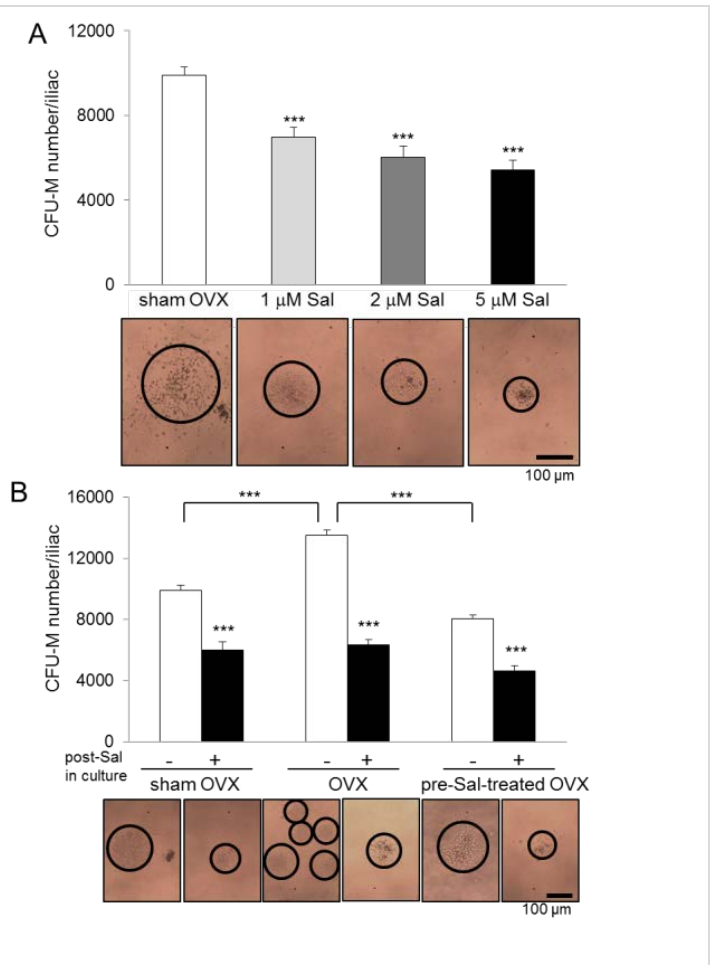
Figure 13. Effects of salubrinal on colony-forming unit-macrophage/monocyte (CFU-M) of BMMNCs. (A) Salubrinal-induced reduction in CFU-M numbers in the sham OVX mice. Salubrinal at 1, 2, and 5 µM or vehicle was post-administered in cells isolated from three groups of mice. A dose-dependent change in the CFU-M number was observed. The images on the bottom exhibit 4 different CFU-M culture conditions, in which the circles indicate the colonies of CFU-M. (B) Comparison of CFU-M numbers among three groups of mice (sham OVX, OVX, and salubrinal treated mice) with and without post administration of salubrinal in culture. Without post-administration of salubrinal the OVX mice presented a larger number of CFU-M colonies than the sham OVX mice, while 4-week salubrinal treatment reduced the CFU-M numbers. The post salubrinal treatment in culture for 7 days reduced the numbers of colonies in all three groups. The representative microphotographs are shown, displaying 6 different conditions in CFU-M cultures with colonies in circle. The results are summary of three independent experiments. Bar = 100 µm. Date represent mean ± s.e.m of ten separate measurements.

The result revealed that cells from the OVX mice had higher rate of migration and adhesion than cells from the sham OVX mice, and salubrinal administration reduced both migration and adhesion of osteoclasts. These results suggest that salubrinal might be useful to block migration and adhesion of cancer cells to bone.

Effects of salubrinal on colony-forming unit-macrophage/monocyte (CFU-M): We also examined the effects of salubrinal on macrophage/monocyte using a colony-forming unit-macrophage/monocyte (CFU-M) assay. Colony-forming unit-macrophage/monocyte (CFU-M) of BMMNCs was assayed using three groups of mice (sham OVX, OVX, and salubrinal-treated OVX mice). BMMNCs were isolated from experimental mice by flushing the iliac bone marrow followed with Ficoll density gradient centrifugation. 2.5×10^4 BMMNCs were seeded onto a 35-mm gridded dish containing methylcellulose supplemented with 30 ng/mL M-CSF and 20 ng/mL RANKL. Cells were incubated at 37°C in a 5% CO_2 incubator for 7 days, and colonies were counted using an inverted light microscope.

Cells isolated from the OVX mice presented an increased number of colonies in the CFU-M assay, while cells from the salubrinal-treated OVX mice showed a decrease in colony numbers (Fig. 13). Furthermore, incubation with salubrinal at 1, 2, or 5 μM showed a dosage dependent decrease in the number of colonies. These results indicate that salubrinal does not stimulate proliferation of pre-osteoclast cells, and thus it contributes to preventing bone resorption by osteoclasts.

Effects of salubrinal on osteoblast differentiation: Besides salubrinal's effects on osteoclasts, we examined its effects on osteoblasts. To induce osteogenic differentiation in the osteoblast differentiation assay, three groups of mice (sham OVX, OVX, and salubrinal-treated OVX mice) MSCs were plated at 2×10^6/ml in osteogenic differentiation medium (MesenCult proliferation kit supplemented with 10^{-8} mol/liter dexamethasone, 50 μg/ml ascorbic acid 2-phosphate, and 10mmol/liter β-glycerophosphate) in 6-well plates. For alkaline phosphatase (ALP) activity assay, cells were maintained in osteogenic differentiation medium for 2 weeks. The medium was changed every other day. For ALP staining, cells were fixed in citrate-buffered acetone for 30 s, incubated in alkaline-dye mix for 30 min, and counterstained with Mayer's Hematoxylin for 10 min. Cells were then evaluated microscopically, and the intensity of ALP staining was recorded. In a CFU-OBL assay that measured activity of alkaline phosphatase (ALP), cells from the salubrinal-treated mice showed an increase in ALP staining. Also, incubation of bone marrow derived cells with salubrinal elevated positive labeling of alkaline phosphatase, %ALP positive (Fig. 14).
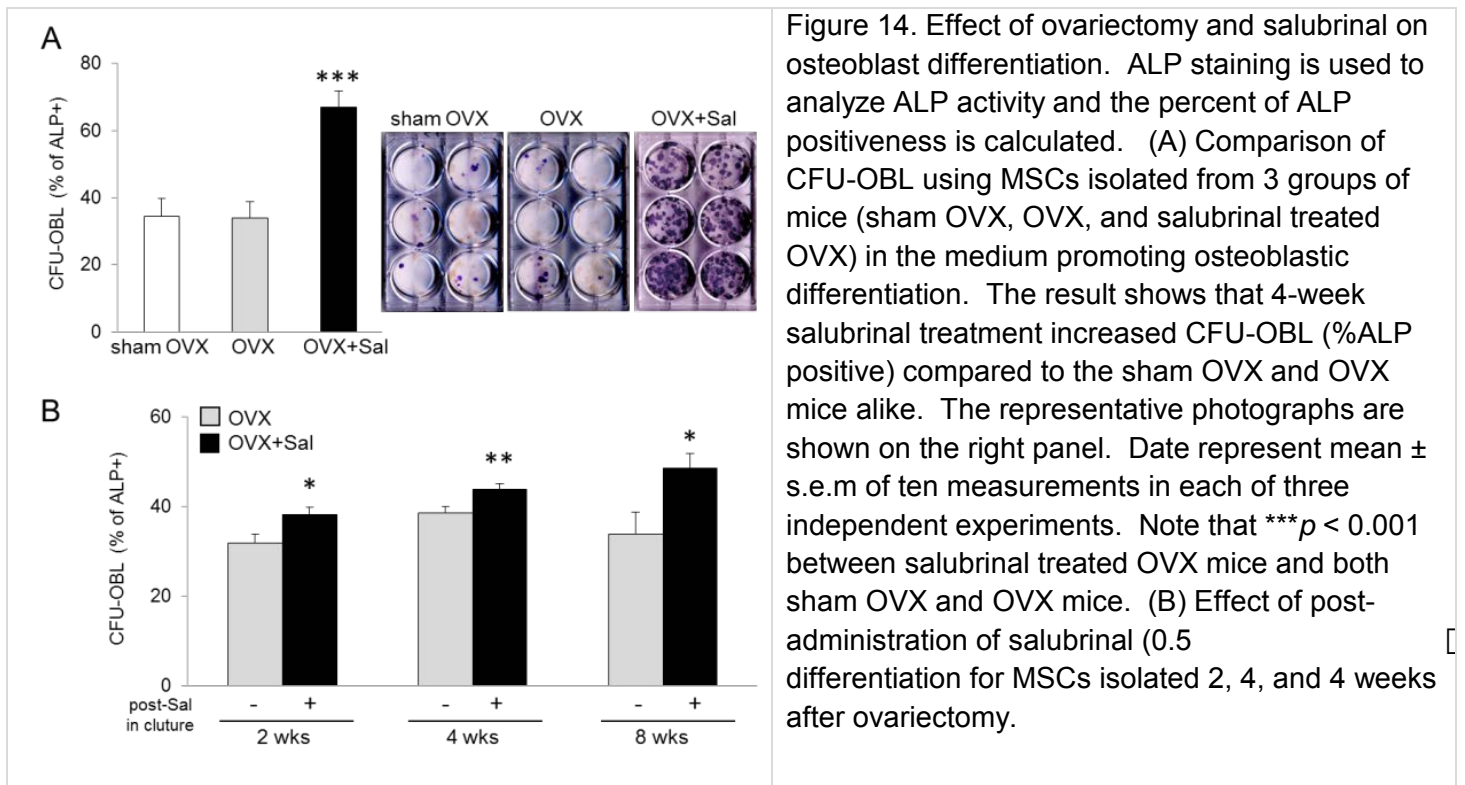

Figure 14. Effect of ovariectomy and salubrinal on osteoblast differentiation. ALP staining is used to analyze ALP activity and the percent of ALP positiveness is calculated. (A) Comparison of CFU-OBL using MSCs isolated from 3 groups of mice (sham OVX, OVX, and salubrinal treated OVX) in the medium promoting osteoblastic differentiation. The result shows that 4-week salubrinal treatment increased CFU-OBL (%ALP positive) compared to the sham OVX and OVX mice alike. The representative photographs are shown on the right panel. Date represent mean ± s.e.m of ten measurements in each of three independent experiments. Note that ***$p < 0.001$ between salubrinal treated OVX mice and both sham OVX and OVX mice. (B) Effect of post-administration of salubrinal (0.5 differentiation for MSCs isolated 2, 4, and 4 weeks after ovariectomy.

Effects of salubrinal on colony-forming unit fibroblasts (CFU-F): The CFU-F assay is a well-established method for the quantification of MSCs from a bone marrow, and it was used for evaluation of the function of MSCs. To measure the frequency of MSCs in bone marrow, the CFU-F assay was performed. Briefly, BMMNCs were separated by Ficoll-Hypaque density gradient centrifugation from bone marrow cells. 2×10^6/ml BMMNCs were plated into 6-well tissue culture plates in triplicate for each condition in 2 ml of complete MesenCult medium and incubated at 37 °C, 5% CO_2. At day 14 of culture, medium was removed from each well followed by two washes of PBS and subsequently stained with HEMA-3 quick staining kit according to the manufacturer's instructions. Colonies with more than 50 cells were counted microscopically at 20× magnification by a phase contrast microscope. Colonies that morphologically differed from MSCs were excluded. The result showed that salubrinal treatment increased frequency of CFU-F compared to both the sham OVX and OVX mice.
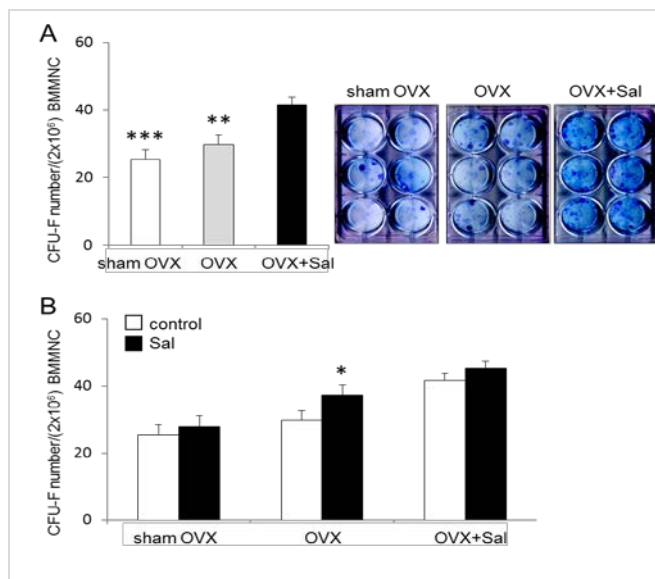

Figure 15. Comparison of CFU-F in 3 groups of mice (sham OVX, OVX, and salubrinal treated OVX). The result shows that 4-week salubrinal treatment increased frequency of CFU-F compared to both the sham OVX and OVX mice. The representative photographs of CFU-F in triplicates stained with HEMA3 are shown on the right panel. Date represents mean ± SEM of 9 - 12 measurements in each of the three independent experiments. Note that ***$p < 0.001$ between salubrinal treated OVX mice and sham OVX and **$p < 0.01$ between salubrinal treated OVX mice and OVX mice.

In vitro effects of salubrinal on osteoclast precursor cells (RAW 264.7 cells): To investigate a mechanism of salubrinal's action on development of osteoclasts, we conducted in vitro analysis using osteoclast precursor cells (RAW 264.7 cells). In a medium for osteoclast development with salubrinal at 0.1 – 20 μM, the protein level of NFATc1 was downregulated in a dose dependent manner (Fig. 16). NFATc1 is a transcription factor that is critically important for osteoclast development. The result indicates that salubrinal is able to reduce the action of NFATc1 through a mechanism, which has not been investigated. There is a possibility that downregulation of NFATc1 is induced by inhibition of NFκB signaling by salubrinal. This possibility is supported by in vitro studies with osteoblasts and chondrocytes (described later in this section), and currently further analysis on NFκB signaling and its linkage to NFATc1 is being conducted.
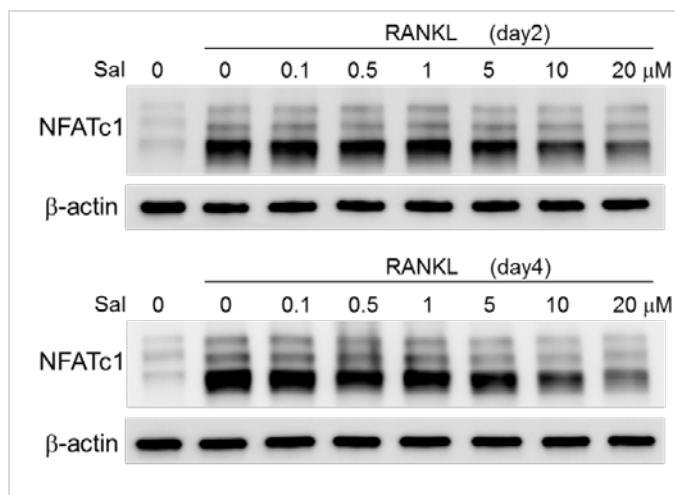

Figure 16. Downregulation of NFATc1 by administration of 0.1 – 20 μM salubrinal. (Top panel) RAW264.7 cells were incubated with salubrinal for 2 days and harvested for protein analysis. (Bottom panel) TRAW264.7 cells were incubated with salubrinal for 4 days and harvested for protein analysis.

In vitro effects of salubrinal on osteoblasts (MC3T3-E1; and clone 14): To identify molecular pathways that mediate stimulatory effects of salubrinal on osteoblast development, we conducted in vitro analysis using

osteoblast cell lines (MC3T3-E1 cells; and its specific clone: MC-14). MC-14 cells have a higher basal level of osteocalcin mRNA expression than MC3T3-E1 cells. Salubrinal is known to block de-phosphorylation of eIF2α (eukaryotic translation initiation factor 2 alpha). It is also known that phosphorylation of eIF2α (p-eIF2α) elevates the protein level of ATF4. As expected, incubation with salubrinal elevated the level of p-eIF2α and ATF4 (Fig. 17).

ATF4 is a transcription factor, necessary for osteoblast differentiation and bone formation, and osteocalcin is one of the markers for osteoblast differentiation. Incubation with salubrinal elevated the mRNA level of osteocalcin in both MC3T3-E1 cells and MC-14 cells (Fig. 18). We further examined the effects of salubrinal on the level of p-NFκB, which indicates activation of NFκB signaling. The result showed that incubation with salubrinal reduced the level of p-NFκB (Fig. 19 left). Furthermore, incubation with salubrinal stimulated alizarin red staining, indicating enhancement of mineralization.
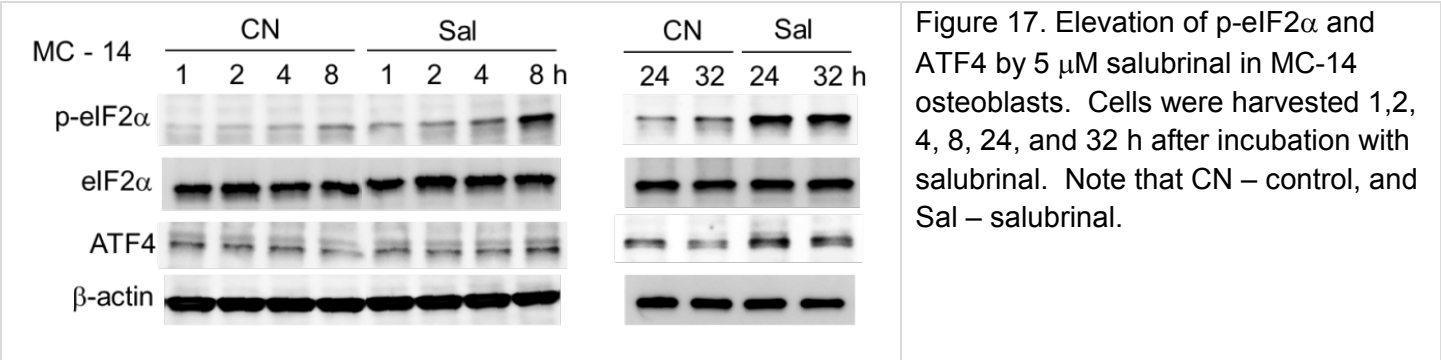

Figure 17. Elevation of p-eIF2α and ATF4 by 5 μM salubrinal in MC-14 osteoblasts. Cells were harvested 1,2, 4, 8, 24, and 32 h after incubation with salubrinal. Note that CN – control, and Sal – salubrinal.
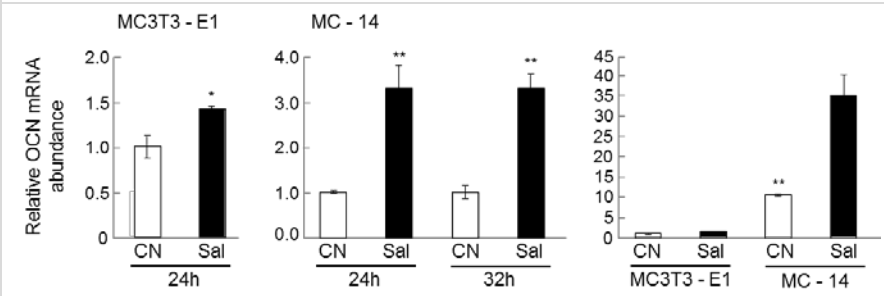
Figure 18. Elevation of osteocalcin mRNA by incubation with 5 μM salubrinal in MC3T3-E1 osteoblast cells and MC-14 cells. Note that the basal level of osteocalcin mRNA in MC-14 is higher than MC3T3-E1 cells.
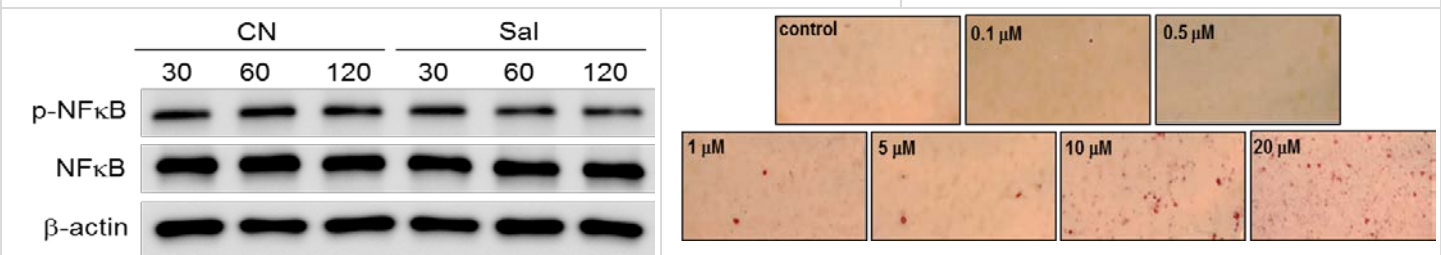
Figure 19. (left) Reduction of p-NFκB in MC-14 cells under incubation with 5 μM salubrinal. Cells were harvested at 30, 60, and 120 min under incubation with salubrinal. (right) Alizarin red staining showing salubrinal driven mineralization of osteoblast culture.

In vitro effects of salubrinal on chondrocytes (C28/I2 cells): Administration of salubrinal may affect not only bone remodeling but also maintenance of joint tissue. Thus, we examined effects of salubrinal on joint cells using C28/I2 chondrocytes. In the first year, we focused on its potential effect on expression and activity of matrix metalloproteinases (MMPs), in particular, MMP13. Incubation with 10 ng/ml TNFα did not significantly alter cell mortality ratio and the total cell numbers regardless of salubrinal administration at 5 or 10 μM (Fig. 20A and 20B). However, treatment with TNFα increased the level of MMP13 mRNA by 2.0 fold and this increase was significantly reduced by application of 5 – 10 μM salubrinal (Fig. 20C). The activity level of MMP13 was increased by TNFα and suppressed by salubrinal (Fig. 20D). TNFα elevated the level of p-p38 MAPK and p-NFκB p65 (Fig. 20E-F). An increase in p-NFκB p65 coincided with an increase in p-IKKα/β and a decrease in IκB, which is an inhibitor of NFκB. In response to 5 μM salubrinal, the levels of p-p38 MAPK, p-IKKα/β, and p-NFκB p65 were decreased at 15 min.

The effects of salubrinal on IL1β-induced upregulation of MMP13 were also medicated by p38 MAPK and NFκB signaling. Cell mortality and cell numbers were not significantly changed (Fig. 21A-B). Compared to the controls in the absence of any other treatment, the level of MMP13 mRNA was increased 2.0 fold by IL1β treatment. Such increase was, however, significantly reduced by 5 - 10 μM salubrinal (Fig. 21C). In the MMP13 activity assay, 10 μM salubrinal reduced IL1β-driven elevation to the basal level lower than that of control cells. The observed increase in the MMP13 mRNA level was accompanied with an elevation of p-p38 MAPK as well as p-NFκB p65 and p-IKKα/β. Furthermore, 10 μM salubrinal reduced the levels of those phosphorylated isoforms for each protein (Fig. 21E-F).
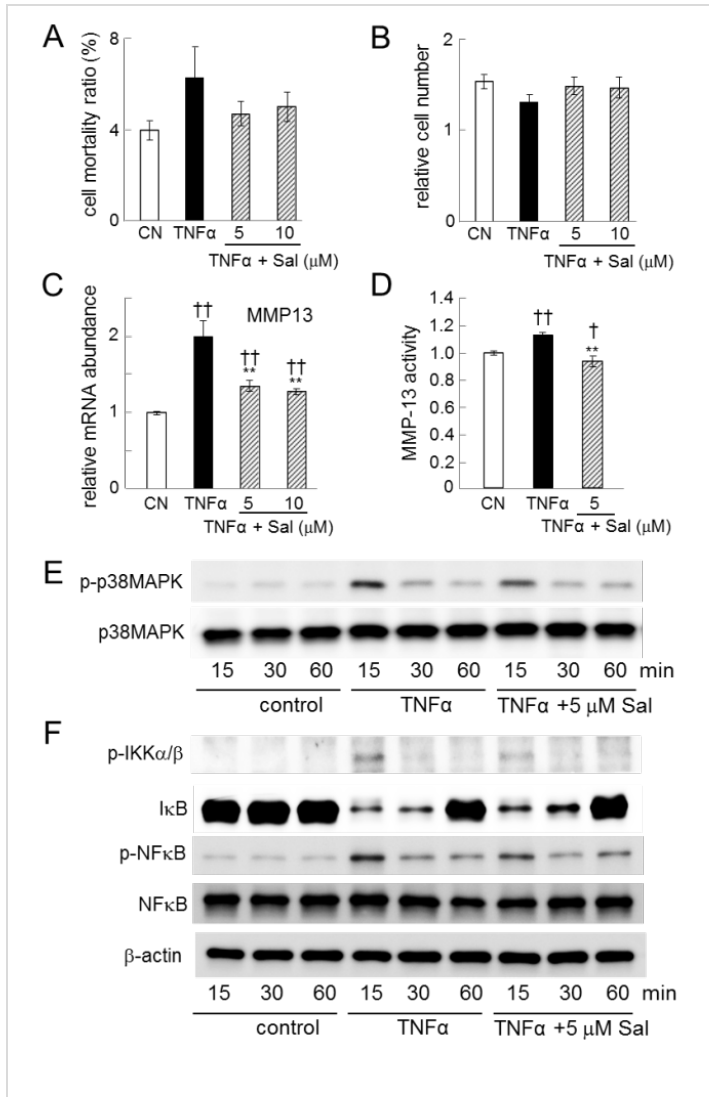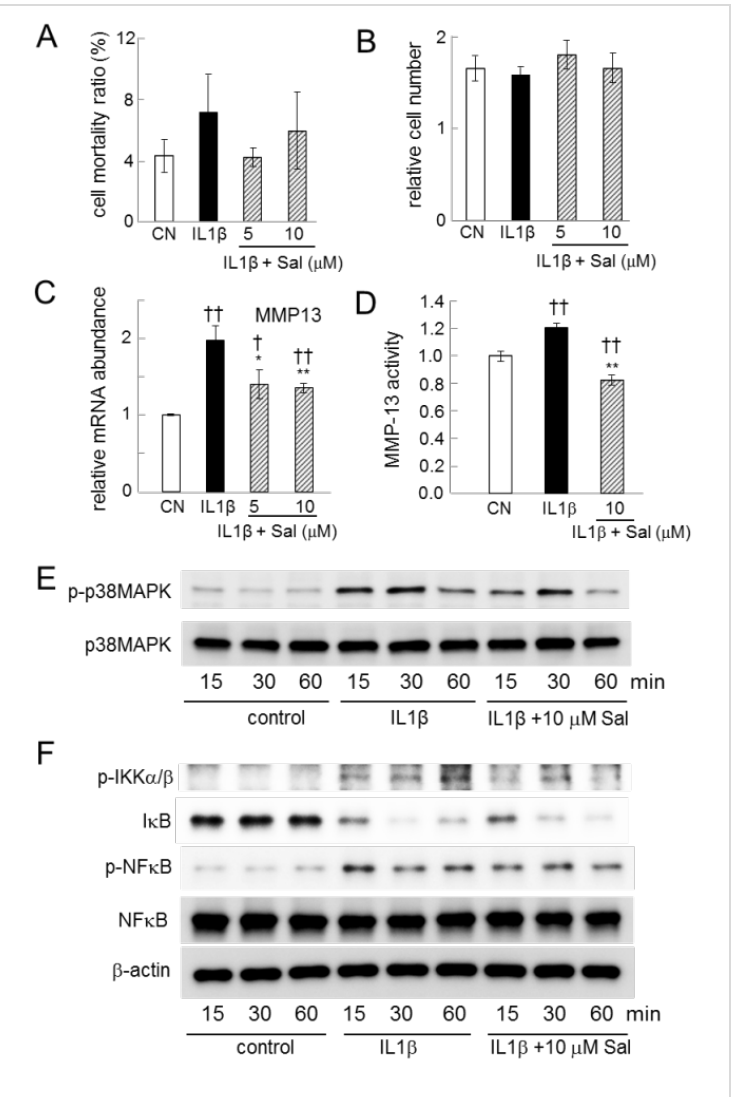

Figure 20. Responses of C28/I2 chondrocytes to TNFα with and without administration of salubrinal. (A) Cell mortality ratio. (B) Relative cell number. (C) Relative MMP13 mRNA abundance in response to TNFα. (D) MMP13 activity. (E) Elevation of p-p38 MAPK by TNFα, which is partially decreased by 5 μM salubrinal. (F) Activation of NFκB by TNFα and partial de-activation by salubrinal.

Figure 21. Responses of C28/I2 chondrocytes to IL1β with and without administration of salubrinal. (A) Cell mortality ratio. (B) Relative cell number. (C) Relative MMP13 mRNA abundance. (D) MMP13 activity. (E) Elevation of p-p38 MAPK by IL1β, which is partially decreased by 10 μM salubrinal. (F) Activation of NFκB by IL1β and its partial suppression by 10 μM salubrinal.

To examine interactions of NFκB signaling to the phosphorylation of p38 MAPK and eIF2α, the protein level of NFκB p65 was significantly reduced by siRNA specific to NFκB p65 (Fig. 22A). Western blot analysis revealed that the effects of silencing NFκB p65 on the level of p-p38 MAPK and p-eIF2α were not detectable (Fig. 22B). In control cells, transfected with negative control siRNA, incubation with TNFα significantly increased MMP13 activity and administration of salubrinal reduced it to the basal level (Fig. 22C). However, cells transfected with

NFκB siRNA showed reduction in TNFα-driven upregulation of MMP13 activity and the effect of salubrinal was not less than that of the control cells (Fig. 22C).

In response to IL1β, treatment at 10 ng/ml, the mRNA levels of MMP1, MMP2, and MMP14 were not altered, but the expression of MMP3 mRNA was elevated. In all cases, administration of salubrinal at 5 or 10 μM did not significantly change their mRNA expression (Fig. 23).
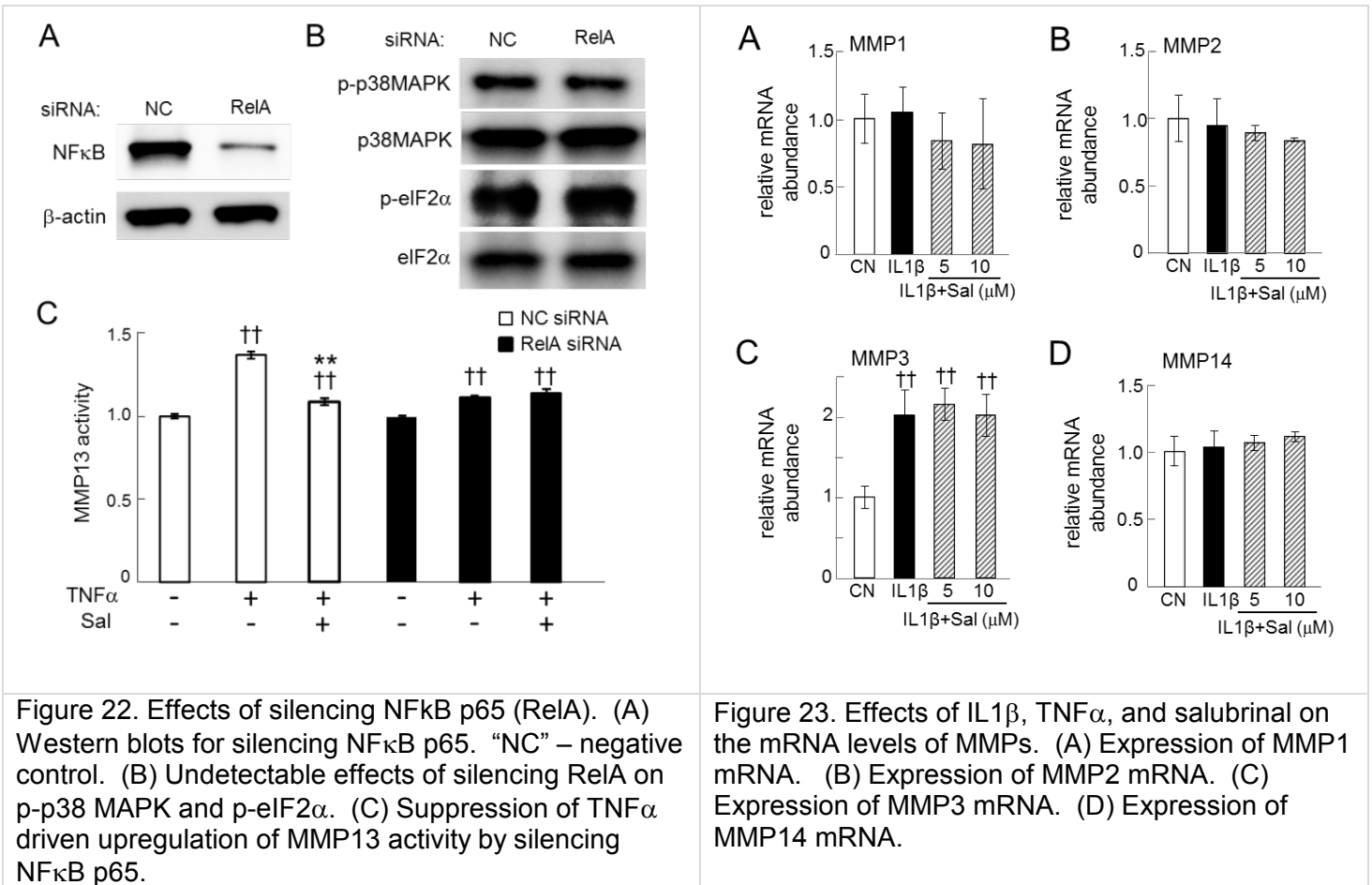

Figure 22. Effects of silencing NFkB p65 (RelA). (A) Western blots for silencing NFκB p65. "NC" – negative control. (B) Undetectable effects of silencing RelA on p-p38 MAPK and p-eIF2α. (C) Suppression of TNFα driven upregulation of MMP13 activity by silencing NFκB p65.

Figure 23. Effects of IL1β, TNFα, and salubrinal on the mRNA levels of MMPs. (A) Expression of MMP1 mRNA. (B) Expression of MMP2 mRNA. (C) Expression of MMP3 mRNA. (D) Expression of MMP14 mRNA.

In this *in vitro* chondrocyte study, the administration of salubrinal suppressed the level of MMP13 mRNA, which was induced by inflammatory cytokines. Salubrinal also decreased cytokine-driven degenerative activity of MMP13. All three inducers in this study (tunicamycin – data not shown, TNFα, and IL1β) elevated the phosphorylation level of p38 MAPK, while the level of p-NFκB p65 was elevated by TNFα and IL1β but not by tunicamycin. Consistent with the involvement of NFκB signaling, salubrinal decreased the level of p-IKK that was known to downregulate the NFκB inhibitor, IκB. Silencing NFκB p65 by RNA interference reduced TNFα-driven upregulation of MMP13 activity, and abolished salubrinal's effect on TNFα.

Collectively, the results demonstrate that salubrinal is capable of attenuating expression and activity of MMP13 by suppressing p38 MAPK and NFκB signaling pathways (Fig. 24).
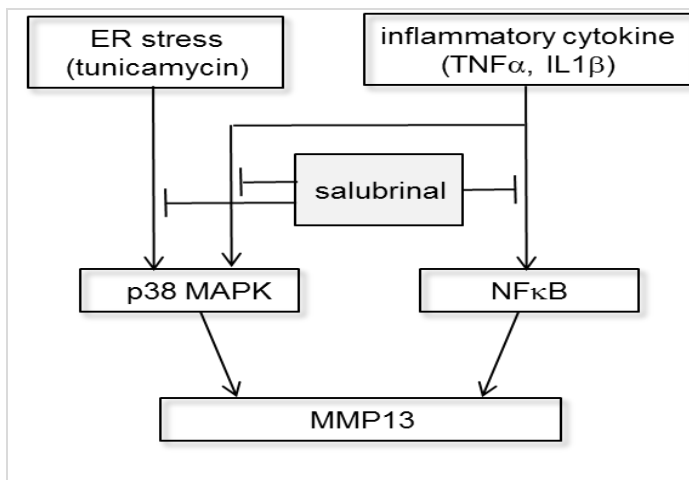
Figure 24. Potential signaling pathways involved in salubrinal administration. Salubrinal is known to elevate the phosphorylated level of elf2α by inhibiting a phosphatase complex specific to eIF2α. However, our investigation in this project indicates that salubrinal affects two other pathways: p38 MAPK and NFκB signaling. We are studying interactions among those signaling pathways and their effects on bone and fat metabolism, in particular, effects on development of bone marrow derived cells, osteoclasts, osteoblasts, and chondrocytes.

Application to chondrosarcoma: Besides osteoporosis and osteoarthritis, we considered a potential application of salubrinal to skeletal malignancies. Approximately one-third of skeletal cancers form chondrosarcoma, making it the second most common form of tumors of bone and cartilage. Few studies have shown efficacy of traditional radiotherapy to chondrosarcoma, and surgical resection remains the main form of treatment. Although proton therapy has recently shown promise as a non-invasive treatment option, it would be desirable to develop a chemotherapeutic procedure that could enhance radiation sensitivity of chondrosarcoma. We examined whether administration of salubrinal would enhance the radiosensitivity of chondrosarcoma. Irradiation with 5 or 10 Gy significantly reduced the number of C28/I2 cells and CW1353 cells on day 5 (Fig. 25). A colony formation (clonogenic survival) assay revealed that reproductive cell survival was reduced by application of radiation and salubrinal in a dose-dependent manner (Fig. 26).
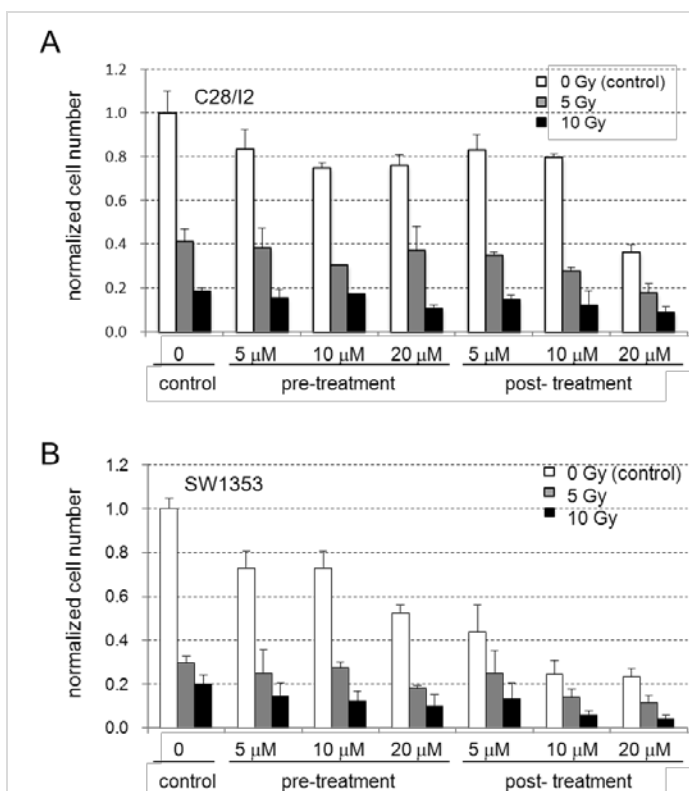

Figure 25. Numbers of live cells after irradiation with 0, 5 or 10 Gy. Cells were pre-treated (pre-treatment) or post-treated (post-treatment) with 0 - 20 μM salubrinal. (A) Number of C28 cells. (B) Number of SW1353 cells.
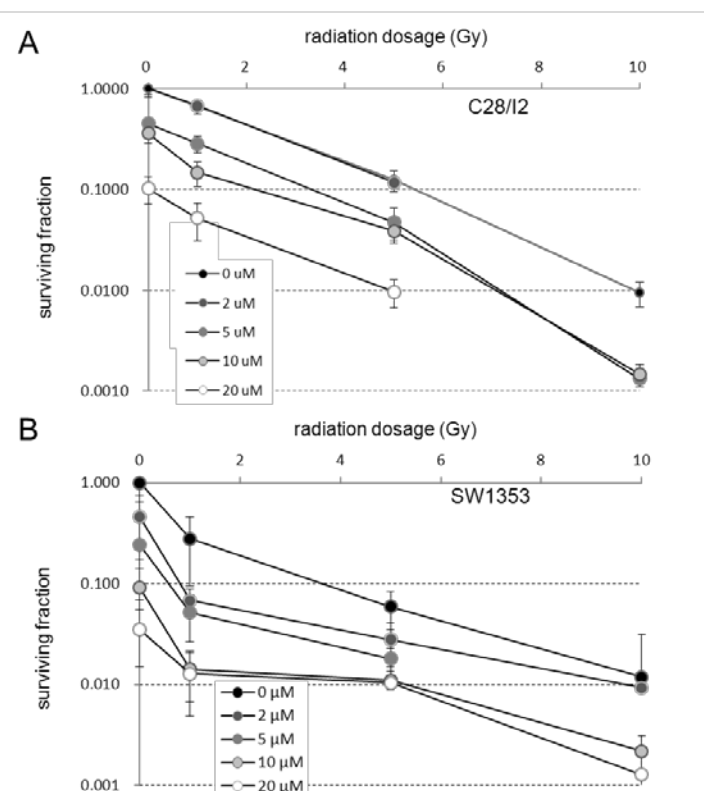
Figure 26. Surviving fraction after simultaneous application of radiation and post-treatment with salubrinal. The normalized number of 1 corresponds to control cells without any treatment. (A) Number of C28 colonies. (B) Number of SW1353 colonies.

Preparation for bone fracture study: One application we will study later in this project is the effects of salubrinal on fracture healing. In the first year, we built an apparatus that will be used for fracture experiments (Figs. 27 and 28).
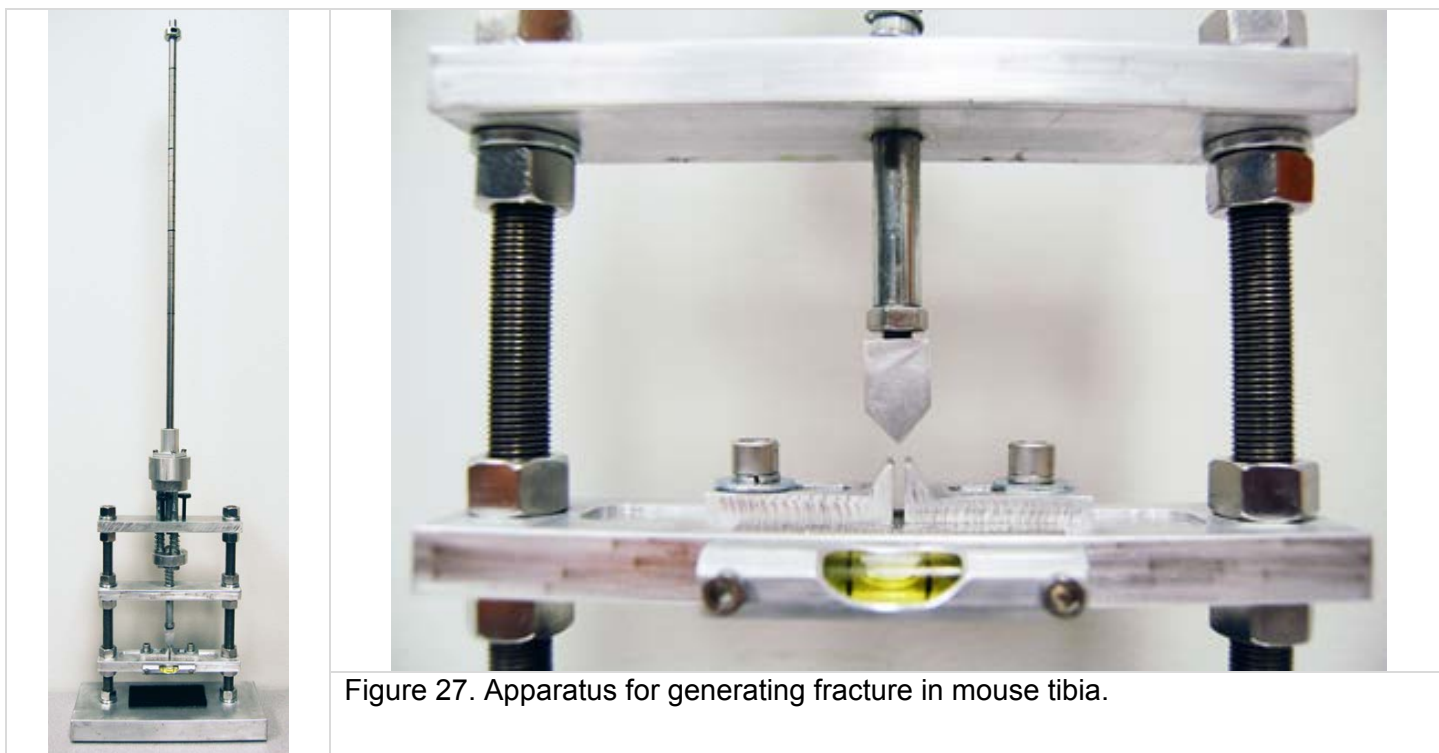

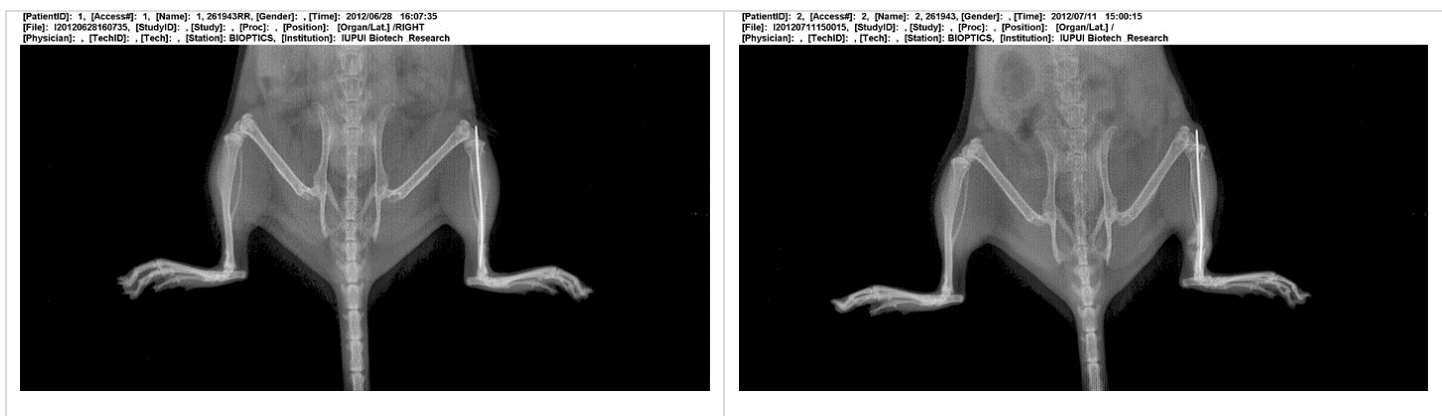Figure 27. Apparatus for generating fracture in mouse tibia.

Figure 28. X-ray images showing bone fracture in the distal tibia.

Preparation for osteonecrosis study (salubrinal and bone cell apoptosis): Preliminary *in vitro* analysis revealed that administration of salubrinal suppressed apoptosis induced by induced by the glucocorticoid dexamethasone (1 µM) or topoisomerase inhibitor etoposide (50 µM) (Fig. 29).

We tested the hypothesis that salubrinal, an inhibitor of complexes that dephosphorylate eukaryotic translation initiation factor 2 subunit α (eIF2α), will affect cell survival, using osteoblastic and osteocytic cell lines and the trypan blue exclusion method. We have previously validated in extensive studies that increased membrane permeability and decreased cell viability measured by trypan blue exclusion represents an accurate measurement of apoptosis as it is inhibited by caspase 3 inhibitors and parallels changes in nuclear morphology and activation of caspases. Cells were plated and cultured at 37°C overnight; then treated with salubrinal or vehicle (dmso) for 1 h prior to addition of the pro-apoptotic agent. After addition of pro-apoptotic agents, cells were harvested and trypan blue was added to a final concentration of 0.04 % to quantify cell viability.
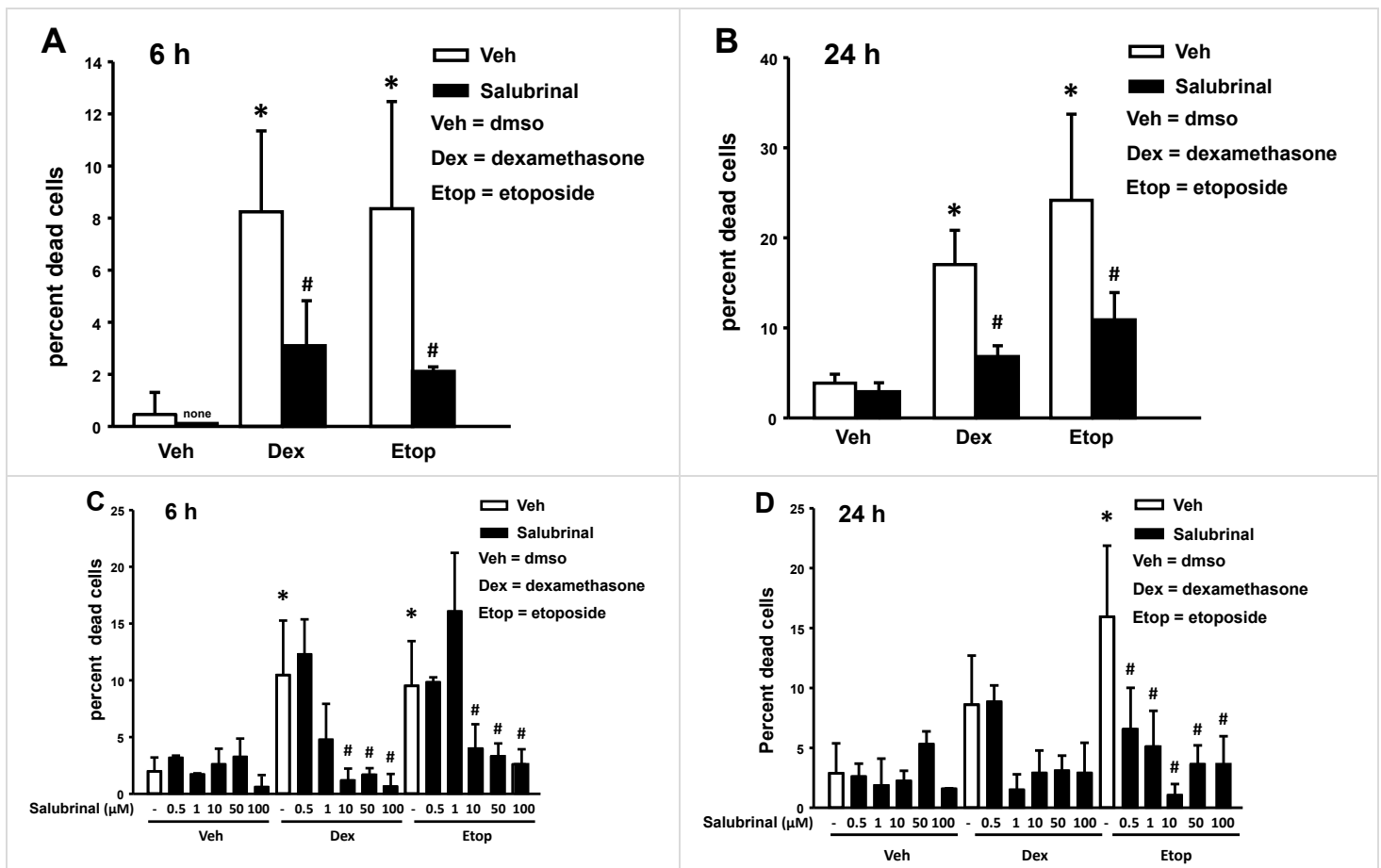
Figure 29: Salubrinal inhibits apoptosis of osteoblastic cells. OB-6 osteoblastic cells were treated for 1 h with vehicle (dmso) or salubrinal, followed by addition of dexamethasone (1 µM) or etoposide (50 µM) for 6 h (A and C), or 24 h (B and D). Cell viability was measured by trypan blue exclusion. The percent dead cells is shown. * $p < 0.05$ versus vehicle-treated cells; # $p < 0.05$ versus cultures treated with the corresponding pro-apoptotic stimulus (dexamethasone or etoposide), by ANOVA.

We found that pretreatment with salubrinal (10 µM) for 1 h protects against cell death induced by the glucocorticoid dexamethasone (1 µM) or topoisomerase inhibitor etoposide (50 µM), measured 6 and 24 h after the addition of the proapoptotic agent to osteoblastic OB-6 cells (Figure 29 A and B). Similar protective effect of salubrinal was observed in osteocytic MLO-Y4 cells (not shown). Dose-response experiments with OB-6 cells from 1 µM to 100 µM demonstrate that the optimal dose at which salubrinal inhibits apoptosis is 10 µM for dexamethasone and etoposide at both 6 and 24h of treatment (Figure 29 C and D), although doses as low as 0.5 µM and as high as 100 µM significantly reduce the percentage of dead cells.

We will continue to determine the effects of salubrinal on steroid induced cell death for future studies on in vivo administration of salubrinal for treatment of steroid induced osteonecrosis.

Preparation for unloading study: The study in the first year showed that salubrinal is effective in preventing bone loss in osteoporosis induced by ovariectomy. We will examine whether salubrinal is effective in preventing bone loss in osteoporosis induced by unloading. Unloading will be simulated by hindlimb suspension, and preliminary data indicate that unloading driven osteoclastogenesis can be suppressed by administration of salubrinal. Preliminary data indicate that unloading-driven loss of BMD in the femur and the lumber spine is partially suppressed by subcutaneous administration of salubrinal (Fig. 30). Furthermore, in bone marrow derived cell culture, the number of adherent pre-osteoclast cells is reduced by post-treatment of salubrinal in three groups of mice (age-matched control, unloading, and salubrinal-treated unloading) (Fig. 31).
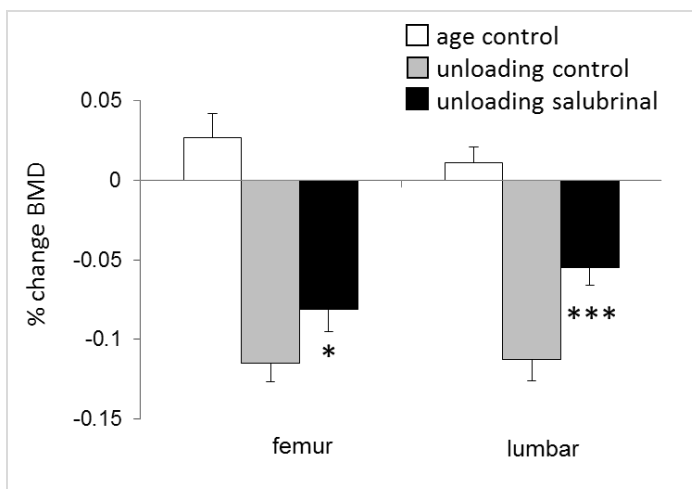
Figure 30. Effects of salubrinal on the femur and lumber spine of the unloaded mice.
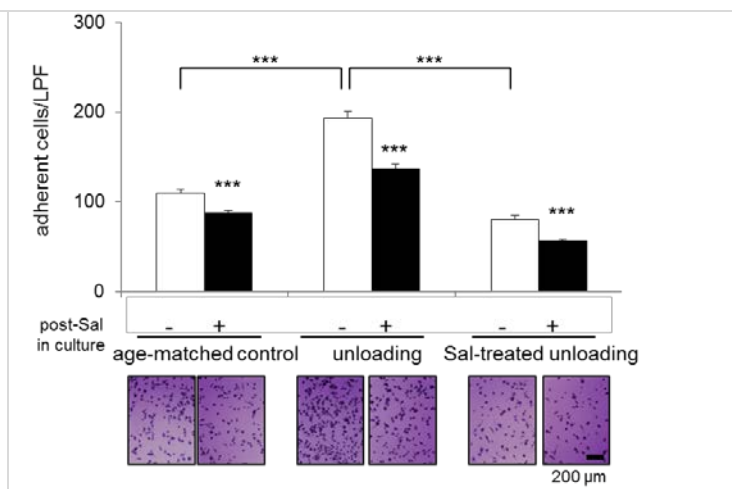

Figure 31. Effects of salubrinal on adhesion of pre-osteoclast cells in unloaded mice.

<u>Communication with Zimmer Co.</u>: As a next step for marketing this agent to orthopedic prosthesis manufactures, PI visited Zimmer Co., one of the largest manufactures of orthopedic prosthesis, in Warsaw, IN in March 2012. Representatives from Zimmer have expressed a high level of enthusiasm in our technology and suggested that we obtain preliminary evaluations as to whether salubrinal can be coated on their prosthesis material, and whether salubrinal-coated grafts would stimulate healing of the bone-graft interface in animal models. PI contacted Dr. Chien-Chi Lin (Assistant Professor of Biomedical Engineering, Indiana University Purdue University Indianapolis - IUPUI) and requested to work for the procedure to coat salubrinal on Zimmer's material (Fig. 32). An internal grant of $35,000 from IUPUI campus was obtained for this purpose and the procedure is now being proposed to Zimmer Co.
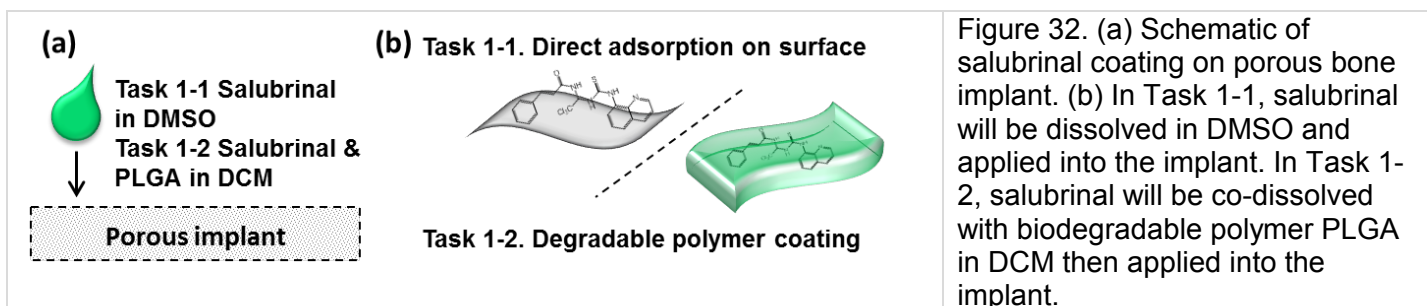

Figure 32. (a) Schematic of salubrinal coating on porous bone implant. (b) In Task 1-1, salubrinal will be dissolved in DMSO and applied into the implant. In Task 1-2, salubrinal will be co-dissolved with biodegradable polymer PLGA in DCM then applied into the implant.

Key Research Accomplishments

In the first year of this project, the key research accomplishments include the followings:

- A formulation for salubrinal (49.5% PEG400 and 0.5% Tween 80) was determined and an effective dosage for *in vivo* (~ 1 mg/kg body weight) and *in vitro* (5 – 20 μM) studies was identified.
- *In vivo* experiments using ovariectomized mice revealed that administration of salubrinal reduces fat weight, and prevents reduction in uterus weight and BMD/BMC.
- *Ex vivo* experiments using bone marrow derived cells showed that salubrinal inhibits osteoclast development and stimulates osteoblast development.
- In vitro experiments using osteoblasts, osteoclasts, and chondrocytes demonstrated that salubrinal regulates transcription factors critical to skeletal metabolism including ATF4, NFκB, and NFATc1.
- A pathway analysis revealed that the observed effects of salubrinal are mediated by eIF2α pathway, p38 MAPK pathway, and NFκB pathway.

Reportable Outcomes

The study in the first year generated the following reportable outcomes.

- Multiple invention disclosures and patents are submitted or being prepared regarding application to cancer therapy, coating to implantable materials, inhibition of MMP13, regulation of bone remodeling and fat metabolism.
- A collaborative relationship was established with Zimmer Co., and a campus research funding of $35,000 was obtained for exploring this collaborative effort.
- Two research abstracts were submitted to the 2013 annual meeting of Orthopedic Research Society (Refs. 1, 2).
- Two peer-reviewed research articles were in press (Refs. 3, 4).
- One peer-reviewed research article was submitted (Ref. 5).

Conclusion

The study in the first year strongly supported the notion that salubrinal can be used for treatment of various skeletal diseases and disorders including osteoporosis, osteoarthritis, and skeletal malignancies. It may have significant effects on regulating fat metabolism and preventing various postmenopausal symptoms. In the first year, we identified significant effects on preventing osteoclastogenesis. Besides the known function of preventing de-phosphorylation of eIF2α, the results strongly suggest that it attenuates p38 MAPK signaling as well as NFκB signaling. In the second year, we will continue our efforts to develop salubrinal as a therapeutic drug for bone and joints and fracture healing.

References

1. Zhang P, Chen A, Dodge T, Tanjung N, Zheng Y, Fuqua C, Yokota H. Salubrinal regulates bone remodeling and fat metabolism in ovariectomized mice. *Abstract to the 2013 annual meeting of Orthopedic Research Society* (submitted).
2. Hamamura K, Hamamura M, Lin CC, Yokota H. Administration of salubrinal attenuates mRNA expression and activity of MMP13 in human chondrocytes. *Abstract to the 2013 annual meeting of Orthopedic Research Society* (submitted).
3. Koizumi Y, Tanjung N, Chen A, Dynlacht JR, Garrett J, Yoshioka Y, Ogawa K, Teshima T, Yokota H. (2012). Administration of salubrinal enhances radiation induced cell death of SW1353 chondrosarcoma cells. *Anticancer Res.* (in press).
4. Zhang P, Hamamura K, Jiang C, Zhao L, Yokota H (2012). Salubrinal promotes wound healing in rat femurs. *J. Bone Miner. Metab.* (in press).
5. Hamamura K, Lin CC, Yokota H. Salubrinal reduces expression and activity of MMP13 in chondrocytes. *Molecular Pharmacology* (submitted).